Journal of Alloys and Compounds 507 (2010) 470–474

Contents lists available at ScienceDirect

Journal of Alloys and Compounds

journal homepage: www.elsevier.com/locate/jallcom

Luminescence of Eu-doped langanite nanopowders synthesized by a citrate sol–gel method

S. Georgescu[a,*], A.M. Voiculescu[a], O. Toma[a], S. Nastase[a], C. Matei[a], M. Osiac[b]

[a] *National Institute for Laser, Plasma and Radiation Physics, 409 Atomistilor Street, Magurele, Jud. Ilfov, 077125, Romania*
[b] *Faculty of Physics, University of Craiova, Romania*

ARTICLE INFO

Article history:
Received 7 June 2010
Received in revised form 23 July 2010
Accepted 27 July 2010
Available online 8 August 2010

Keywords:
Langanite
Nanopowder
Sol–gel
Eu^{3+}
Luminescence

ABSTRACT

Eu-doped langanite nanopowders were prepared by a citrate sol–gel method and annealed in air at various temperatures between 700 °C and 1000 °C. For annealing temperatures up to 800 °C, only the langanite phase is observed. For higher annealing temperatures, part of the langanite powder transforms in perovskite ($LaGaO_3$), as evidenced in both XRD and luminescence spectra. Regardless the annealing temperature, the lifetime of $^5D_0$ remains close to 1 ms. The reddish color of the powders due to color centers associated to oxygen defects intensifies with increasing annealing temperature. The best efficiency of the Eu-langanite nanopowders was obtained for the sample annealed at 700 °C (~60% of the efficiency of the bulk material).

1. Introduction

The search of new and efficient phosphors for solid-state lighting is a problem of great interest in present. One of the problems to be solved is the improvement of the spectral matching between the emission of the LED and the absorption of the phosphor. Though efficient, the rare-earth doped phosphors present narrow absorption lines in near UV or blue where efficient LEDs are available. A possible solution is the use of partially disordered crystals as hosts for rare-earth ions. As a result of the disorder, the absorption lines are wider. Such hosts could be the crystals from the langasite family (generic—LGX), namely langasite (LGS—$La_3Ga_5SiO_{14}$), langanite (LGN—$La_3Ga_{5.5}Nb_{0.5}O_{14}$) and langatate (LGT—$La_3Ga_{5.5}Ta_{0.5}O_{14}$).

LGS, LGN and LGT crystallize in the *P321* space group, symmetry class *32* and are isostructural with the calciumgallogermanate ($Ca_3Ga_2Ge_4O_{14}$) [1]. The general formula is $A_3BC_3D_2O_{14}$ where *A* represents the dodecahedral positions (distorted Thompson cubes), *B* represents the octahedral positions and *C* and *D* represent the tetrahedral positions. La^{3+} occupies the position *A*. The local symmetry at this site is C_2 [2]. In contrast with LGS where Ga^{3+} and Si^{4+} share with equal probability the tetrahedral positions *D*, in LGN (LGT) the octahedral positions *B* are occupied by two different ions, Ga^{3+} and Nb^{5+} (Ta^{5+}) (also, with equal probability). Ga^{3+} occupies the remaining positions (*C* and *D*). The structural difference between LGS and LGN (or LGT) consists in the placement of the shortest distance positions randomly occupied around the *A* site: four *D* positions in the plane perpendicular on the C_2 axis for LGS and two *B* positions along the C_2 axis in LGN and LGT. Besides, there is a larger charge difference between Nb^{5+} (or Ta^{5+}) and Ga^{3+} than between Si^{4+} and Ga^{3+} [3,4].

When excited in the near UV (395 nm, transition $^7F_0 \rightarrow {}^5L_6$), Eu^{3+}-doped LGX crystals show bright red luminescence which suggests the possibility to use these materials as red phosphors. The luminescence properties of LGS, LGT, and LGN Eu-doped crystals were discussed in Refs. [3–7].

Obtaining the powder of LGX starting with single crystal growth and subsequent milling is a rather expensive approach. Other methods resulting directly in powders would be of interest. Such a method, involving lower temperature synthesis, is the sol–gel approach. There are only few papers regarding the sol–gel synthesis of LGX compounds [8–12] and only one (in our best knowledge) concerning Eu-doped nanopowder (Eu-doped LGN) [9]. In Ref. [9] the as-obtained Eu-doped LGN powder is annealed at temperatures between 800 °C and 1100 °C for 5 h and no phase transition was observed.

In this paper, encouraged by the previous results (ours and from the literature), we synthesized, using the citrate sol–gel method described in Refs. [9–11], Eu-doped LGN nanopowders. The effect of thermal treatments is examined using XRD and optical spectroscopy (diffuse reflectance and luminescence spectra, kinetics of

---

[*] Corresponding author at: National Institute for Laser, Plasma and Radiation Physics, Solid-State Quantum Electronics Laboratory, 409 Atomistilor Street, 077125 Magurele, Ilfov, Romania.
E-mail address: serban.georgescu@inflpr.ro (S. Georgescu).

0925-8388/$ – see front matter © 2010 Elsevier B.V. All rights reserved.
doi:10.1016/j.jallcom.2010.07.206

the luminescent levels $^5D_0$ and $^5D_1$). A comparison is made with the results obtained on crystalline Eu:LGN [7].

2. Experimental

The Eu (3 at.%)-doped LGN powder was obtained using the citrate sol–gel method [9–11]. For preparing the nanoparticles, $La(NO_3)_3{\cdot}6H_2O$, $Ga(NO_3)_3{\cdot}5H_2O$, $Eu(NO_3)_3{\cdot}6H_2O$, $Nb(OH)_5$ and citric acid were used as precursors, in the corresponding ratios. First of all, $Nb(OH)_5$ was synthesized by fully dissolving Nb_2O_5 in HF, followed by the addition of ammonia. The white powder of $Nb(OH)_5$ was then dissolved in an aqueous solution of citric acid. The resulting sol was stirred until a clear solution has been achieved. Then, an aqueous mixture containing La^{3+}, Ga^{3+} and Eu^{3+} nitrates has been added to the Nb-citrate system, with constant stirring. The final solution was stirred for another 1 h, heated in an oven at 80 °C, until a very viscous gel has been formed. The brown-yellow colloid was dried at 110 °C, and then calcined in air at temperatures between 700 °C and 1000 °C.

XRD measurements were performed on a Shimadzu 6000 diffractometer (Cu Kα). The fluorescence of the Eu:LGN was excited using a ScienceTech Xe-Hg 350-W lamp with suitable filters. The fluorescence spectra were measured at room temperature using a Horiba Jobin-Yvon 1000M monochromator, an S-20 photomultiplier and an SR830 lockin amplifier from Stanford Research Systems. For decay measurements, the luminescence was excited with the second harmonics of a Nd-YAG laser and analyzed with an Ortec MCS-PCI multichannel scaler card. The experimental setup for diffuse reflectance measurements was described elsewhere [5]. All measurements were performed at room temperature.

3. Results and discussion

In Fig. 1 are shown the XRD patterns for Eu-doped LGN powders annealed at 800 °C and 1000 °C. For comparison, the XRD pattern of the powder obtained by milling a Eu-doped LGN single crystal is also shown. For the sample annealed at 800 °C, all the observed diffraction lines belong to the LGN phase. For higher annealing temperatures (1000 °C), besides the diffraction lines corresponding to the LGN phase, other diffraction lines, identified as belonging to $LaGaO_3$ phase are observed (denoted with stars in Fig. 1). It results that for the Eu-LGN powders obtained using this sol–gel method, the LGN phase is not stable at higher annealing temperatures and transforms in $LaGaO_3$, possibly due to the evaporation of gallium oxide. No such transformation was noted in Refs. [8–12].

The Scherrer formula enables the calculation of the average size of the coherence domain of the LGN grains. For the sample treated at 800 °C, the size of the coherence domain is about 90 nm, while for the sample annealed at 1000 °C it increases to 160 nm. The calculations were carried off using the two most intense diffraction lines around $2\theta = 30°$, both characteristic to the LGN phase.

The luminescence spectrum (Fig. 2) shows the lines originating in ^5D_J levels ($J = 0$, 1, and 2). The fluorescence was excited at 395 nm (transition $^7F_0 \rightarrow {}^5L_6$). Since the sensitivity of our experimental apparatus is higher for higher wavenumbers, in order to see better the luminescence lines from $^5D_1$ and $^5D_2$ levels, the spectra in Fig. 2 were not corrected for the spectral sensitivity. As one can see, the main luminescent transition is $^5D_0 \rightarrow {}^7F_2$ (at ~16,250 cm^{-1}). No significant modification in the shape of the luminescence spectrum is observed when the annealing temperature increases from 700 °C to 800 °C. For higher temperatures, the luminescence spectra reflect the transition from pure LGN phase to the mixture between LGN and $LaGaO_3$ phases. The modifications are evident in the luminescence bands corresponding to $^5D_0 \rightarrow {}^7F_1$ and $^5D_0 \rightarrow {}^7F_2$ transitions. For example, the luminescence peak at 16,925 cm^{-1} (~590 nm), which dominates the $^5D_0 \rightarrow {}^7F_1$ transition in the luminescence spectrum of the sample annealed at 1000 °C, is characteristic for Eu^{3+} in $LaGaO_3$ [13].

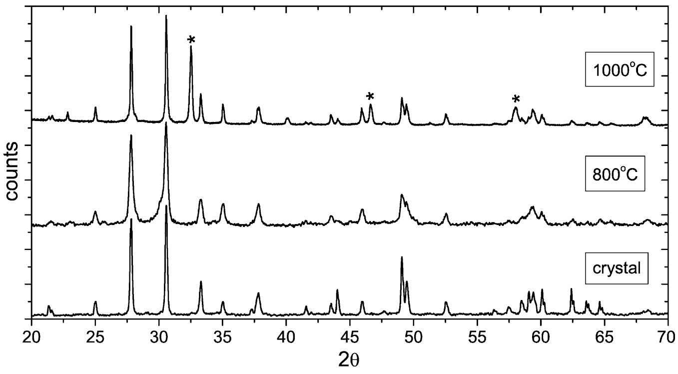

Fig. 1. XRD patters for Eu-doped powders annealed for five hours in air at 800 °C and 1000 °C as well as of the Eu:LGN crystal powder. The diffraction lines denoted by * belong to the $LaGaO_3$ phase.

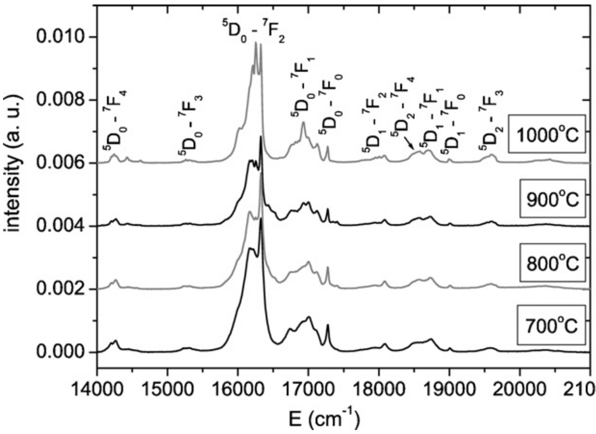

Fig. 2. Luminescence spectra of Eu-doped LGN powders annealed at various temperatures. The spectra are not corrected for spectral sensitivity of the experimental apparatus. The main transitions are indicated.

The diffuse reflectance spectra (in rapport with the 'white' $BaSO_4$) of the Eu-LGN samples are given in Fig. 3. The absorption lines corresponding to the transitions from $^7F_0$ and $^7F_1$ (populated at room temperature) are visible. The baselines of the diffuse reflectance spectra are tilted towards shorter wavelengths, more tilted for higher annealing temperatures (i.e. the reddish coloration of the samples is intensified with the annealing temperature). The red coloration of the crystals from the langasite family is related to point defects involving oxygen [14–16].

The thermal treatments could modify the neighborhood of the Eu^{3+} ion. In order to estimate the asymmetry ratio R_2, defined as the ratio between the area of the electric-dipole transition ($^5D_0 \rightarrow {}^7F_2$) and the area of the magnetic-dipole one ($^5D_0 \rightarrow {}^7F_1$), the fluorescence spectra should be corrected for the spectral sensitivity of the experimental apparatus and the superposition with the luminescence lines from $^5D_1$ and $^5D_2$ should be eliminated. This elimination, performed by adjusting the phase of the lockin amplifier, is possible due to the large difference between the lifetime of $^5D_0$ (close to 1 ms) and lifetimes of the higher levels (tens of microseconds), as obtained from the decay measurements. The results are shown in Fig. 4. Since the areas of the $^5D_0 \rightarrow {}^7F_{5,6}$ transitions are very small [7], only $^5D_0 \rightarrow {}^7F_J$ ($J = 0$, 1, 2, 3, and 4) lines are shown. We obtained $R_2 = 5.13 \pm 0.02$ for the sample annealed at 700 °C and 5.06 ± 0.02 for the sample annealed at 800 °C. For the Eu-LGN powder obtained by milling the single crystal, $R_2 = 4.68 \pm 0.02$ [7]. The reduction of the asymmetry ratio with the annealing temperature is related to the improving of the local symmetry produced by the increase of the particle size. For higher annealing temperature part of the LGN particles transforms in $LaGaO_3$ which has a different local symmetry (C_s) at the Eu^{3+} position [17].

As a measure of the luminescence efficiency, we represented the total areas of the luminescence spectra of the powders function of the annealing temperature; the area of the luminescence

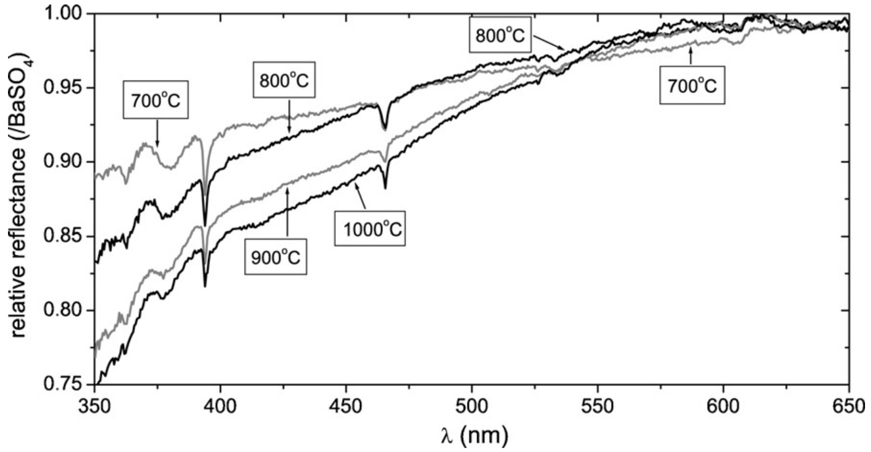

Fig. 3. Reflectance spectra of Eu-doped LGN powders annealed at various temperatures.

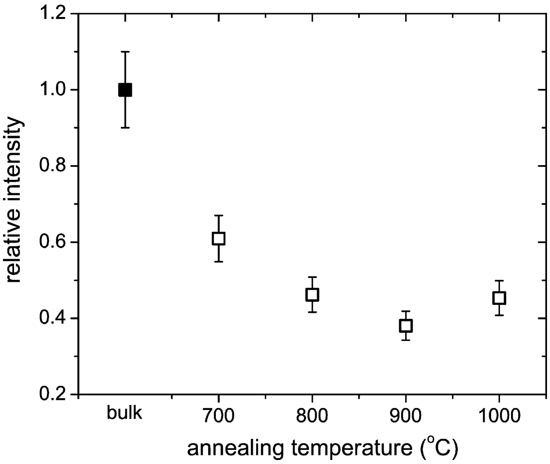

Fig. 5. Luminescence intensity (area of the luminescence spectra) of the Eu:LGN powders function of the annealing temperature; for comparison, the area of the luminescence spectrum of the bulk material (normalized to unity) is also given.

spectrum of the bulk material (obtained by milling the single crystal) is also shown. The represented areas were normalized to the area of the bulk material luminescence spectrum. We note that the Eu-concentration is the same in the nanopowders and in the bulk: 3 at.% in rapport with La. In order to obtain reproducible results from the comparison of the luminescence spectra areas, a mechanically stable experimental setup was designed; the powder samples were placed in the same position at every measurement, and their density was maintained the same. The results are given in Fig. 5. Every experimental point in this figure represents an average of several measurements.

The efficiency of the nanopowders is inferior to the bulk material. The best result was obtained for the sample annealed at 700 °C. Usually, the efficiency increases with the temperature of the thermal treatment due to the improvement of the crystallinity and the removal of the adsorbed impurities. The decrease of efficiency with annealing temperature observed in this case could be related to the reddish color of the powders. This color which intensifies with the temperature of the thermal treatment screens the pump radiation, reducing the absorption of the UV light, decreasing the emission intensity. The increase in intensity of the red coloration is stronger in the temperature range 700–900 °C and weaker between 900 °C and 1000 °C (see Fig. 3). Thus, in the range 900–1000 °C the decrease of the efficiency due to the red coloration can, in principle, be compensated by the favorable effect of the elimination of adsorbed impurities and improvement of crystallinity. The competition of these factors is complicated in this case by the transformation of LGN in perovskite.

The decay curves of the $^5D_0$ level for pumping in $^5D_1$ (pump transition $^7F_1 \rightarrow {}^5D_1$) for the samples annealed at 700 °C and 800 °C

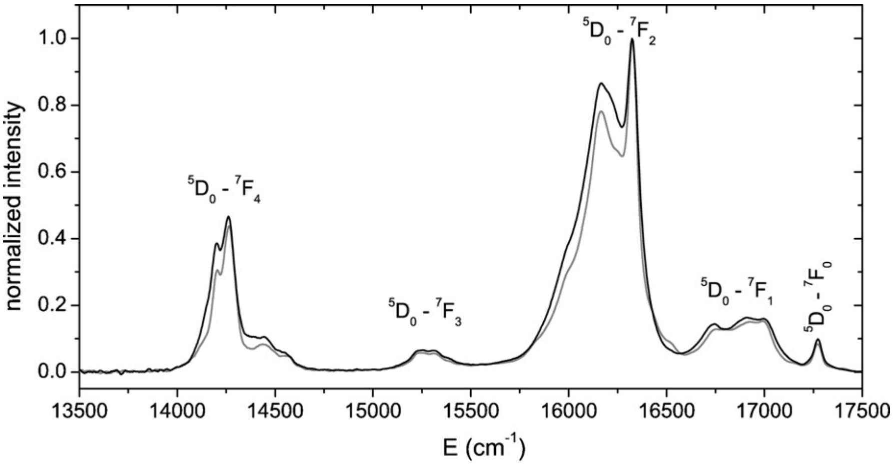

Fig. 4. Luminescence spectra of the samples annealed at 700 °C (black line) and 800 °C (gray line). The spectra were corrected for the spectral sensitivity of the experimental apparatus and the superposition with the lines from higher ^5D_J levels was eliminated by adjusting the phase of the lockin amplifier.

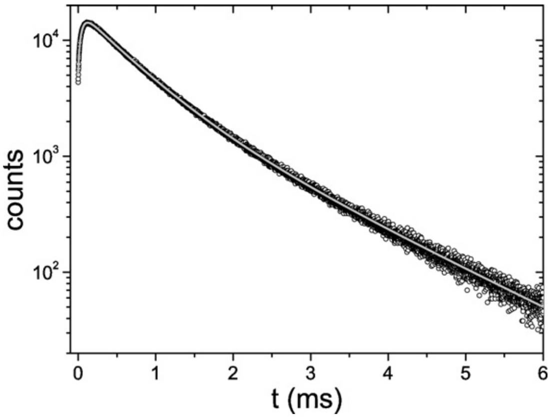

Fig. 6. Decay curve for the luminescence of $^5D_0$ level in Eu-doped LGN powders annealed at 700 °C. The risetime is due to the lifetime of the $^5D_1$ level. Black circles: experiment; continuous gray line: three-exponential fit.

are given in Figs. 6 and 7. The risetime observed in Figs. 6 and 7 is due to the lifetime of $^5D_1$.

The decay of $^5D_0$ can be very well fitted with a three-exponential expression

$$I(t) = I_1 \exp\left(\frac{-t}{\tau_1}\right) + I_2 \exp\left(\frac{-t}{\tau_2}\right) + I_3 \exp\left(\frac{-t}{\tau_3}\right) \qquad (1)$$

with the first exponential corresponding to the rising part of the curve ($I_1 < 0$) and the last two mimicking its falling part. The values of I_2, τ_2, I_3, τ_3 can be used to calculate the 'efficiency' lifetime according to $\tau_{eff} = (I_2\tau_2 + I_3\tau_3)/(I_2 + I_3)$ which results directly from the definition of the 'efficiency' lifetime.

We obtained the following results: $\tau_{eff}(^5D_0) = 760\ \mu s$ for the sample annealed at 700 °C and $\tau_{eff}(^5D_0) = 930\ \mu s$ for the sample annealed at 800 °C. Our results are in the millisecond domain and very different from the lifetime obtained in Ref. [9] (9.2 ns). For the present time, we are not able to explain this difference.

The radiative lifetime can be obtained from the calibrated luminescence spectra given the probability of the magnetic-dipole transition [18]. However, the calculation of the magnetic-dipole transition probability would require the knowledge of the refractive index of the sample. For the case when the crystallites size is smaller than the radiation wavelength, an average refractive index (between the refractive indexes of the crystal and the medium) was introduced [19]. This average index of refraction depends on the compactness of the powder and on the tendency of its particles to agglomerate; it is therefore difficult to find its value.

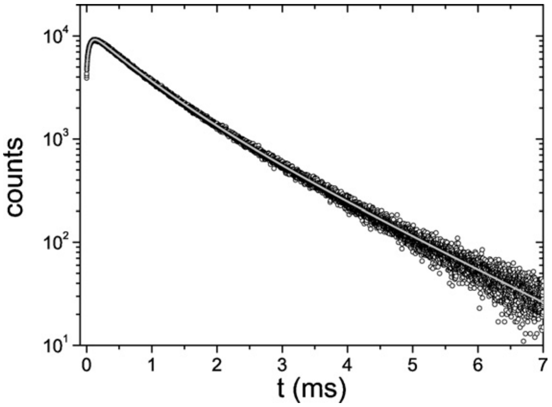

Fig. 7. Decay curve for the luminescence of $^5D_0$ level in Eu-doped LGN powders annealed at 800 °C. The risetime is due to the lifetime of the $^5D_1$ level. Black circles: experiment; continuous gray line: three-exponential fit.

From the risetime of the $^5D_0$ decays, the lifetime of the $^5D_1$ level can be estimated. For both samples its value is approximately 50 μs. For the Eu-LGN samples annealed at higher temperatures, though part of the material transforms in $LaGaO_3$, the lifetimes do not change significantly: 930 μs and 67 μs for the sample annealed at 900 °C and 845 μs and 64 μs, for the 1000 °C sample. The non-exponential character of the $^5D_0$ decay could be due to the nonuniformity of the sites occupied by Eu^{3+} ions in nanocrystallites and to the influence of the impurities still present on the grain surfaces. For the bulk Eu:LGN [7], the decay of $^5D_0$ is exponential with $\tau = 1050\ \mu s$; the efficiency lifetime for $^5D_1$ is 63 μs, not far from the values obtained for sol–gel samples.

4. Conclusions

Eu-doped LGN powders were obtained from a citrate sol–gel synthesis and thermally treated at temperatures between 700 °C and 1000 °C. For the annealing temperatures up to 800 °C, only the langanite phase is observed. For higher annealing temperatures, part of the langanite transforms in $LaGaO_3$. The modifications are visible in both XRD and luminescence spectra. Besides the luminescence of $^5D_0$, luminescence from higher ^5D_J levels is observed in the luminescence spectra. The asymmetry ratio decreases from 5.13 ± 0.02 for the sample annealed at 700 °C to 5.06 ± 0.02 (800 °C) denoting the improvement of the local symmetry with the increase of the particles' size.

For pumping in the $^5L_6$ level (395 nm), the greatest efficiency of the emission of Eu:LGN powders was obtained for the sample treated at 700 °C. The efficiency obtained represented about 60% of the bulk material efficiency.

As a result of thermal treatment in air, the Eu-doped LGN powders become reddish, the coloration being intensified for higher temperatures.

For annealing temperatures between 700 °C and 1000 °C the lifetime of $^5D_0$ level remains in the millisecond domain while the lifetime of $^5D_1$ varies from 50 μs to 67 μs.

Acknowledgement

This work was supported by the National Council of the Scientific Research in Universities (CNCSIS) in the frame of the Project (IDEI) ID 812.

References

[1] B.V. Mill, A.V. Butashin, G.G. Kodzhabagian, E.L. Belokoneva, N.V. Belov, Doklady Akademii Nauk SSSR 264 (1982) 1385.
[2] V.N. Molchanov, B.A. Maksimov, A.F. Kondakov, T.S. Chernaya, Yu.V. Pisarevsky, V.I. Simonov, JETP Lett. 74 (2001) 222.
[3] S. Georgescu, O. Toma, A.M. Chinie, L. Gheorghe, A. Achim, A.S. Stefan, Opt. Mater. 30 (2008) 1007.
[4] S. Georgescu, O. Toma, A.M. Chinie, L. Gheorghe, A. Achim, A.S. Stefan, J. Lumin. 128 (2008) 741.
[5] S. Georgescu, A.M. Voiculescu, O. Toma, C. Tiseanu, L. Gheorghe, A. Achim, C. Matei, Optoelectron. Adv. Mater.–Rapid Commun. 3 (2009) 1379.
[6] S. Georgescu, A.M. Voiculescu, C. Matei, O. Toma, L. Gheorghe, A. Achim, Romanian Rep. Phys. 62 (2010) 128.
[7] S. Georgescu, O. Toma, A.M. Voiculescu, L.Gheorghe, A. Achim, C. Matei, S. Hau, to be published.
[8] X.Q. Zhang, D.R. Yuan, S. Guo, J. Crystal Growth 308 (2007) 80.
[9] F.P. Yu, D.R. Yuan, X. Zhao, S.Y. Guo, X.L. Duan, L.M. Kong, X.Q. Wang, J. Crystal Growth 310 (2008) 3256.
[10] F.P. Yu, D.R. Yuan, X.L. Duan, L.M. Kong, X.Z. Shi, S.Y. Guo, L.H. Wang, X.F. Cheng, X.Q. Wang, J. Alloys Compd. 459 (2008) L1.
[11] F.P. Yu, D.R. Yuan, L.M. Kong, X.L. Duan, S.Y. Guo, X.Q. Wang, X. Zhao, Nanotechnology 19 (2008) 045705.
[12] F.P. Yu, D.R. Yuan, S.Y. Guo, X.L. Duan, X.Q. Wang, L.M. Kong, X.Q. Zhang, X. Zhao, Cryst. Res. Technol. 43 (2008) 522.
[13] X. Liu, J. Lin, J. Appl. Phys. 100 (2006) 134306.

[14] T. Taishi, T. Hayashi, N. Bamba, Y. Ohno, I. Yonenaga, K. Hoshikawa, Physica B 401–402 (2007) 437.

[15] T. Taishi, T. Hayashi, T. Fukami, K. Hoshikawa, I. Yonenaga, J. Crystal Growth 304 (2007) 4.

[16] G.M. Kuzmicheva, E.N. Domoroschina, V.B. Rybakov, A.B. Dubovsky, E.A. Tyunina, J. Crystal Growth 275 (2005) e715.

[17] I. Garcia-Rubio, J.A. Pardo, R.I. Merino, R. Cases, V.M. Orera, J. Lumin. 86 (2000) 147.

[18] M.H.V. Werts, R.T.F. Jukes, J.W. Verhoeven, Phys. Chem. Chem. Phys. 4 (2002) 1542.

[19] R.S. Meltzer, S.P. Feofilov, B. Tissue, H.B. Yuan, Phys. Rev. B 60 (1999) R14012.